



FUZZY MODAL PARAMETERS

G. PLESSIS, B. LALLEMAND, T. TISON AND P. LEVEL

*Laboratoire d'Automatique et de Mécanique Industrielles et Humaines, Groupe Génie Mécanique,
UMR CNRS 8530, Université de Valenciennes, BP 311, 59 304 Valenciennes Cedex, France*

(Received 4 June 1999, and in final form 8 November 1999)

In order to identify modal parameters with uncertain experimental data, a non-deterministic identification method based on fuzzy formalism is proposed. The aim is to provide a degree of confidence in the modal parameters identified.

© 2000 Academic Press

1. INTRODUCTION

A structure's modal parameters can be determined by an analytical or experimental approach. The results of the two methods show differences that can be attenuated by modal updating techniques. In the traditional modal updating approach, the experimental data is considered to be error free with the totality of the error said to come from the model. This hypothesis is obviously erroneous because, whether identified or not, there are several sources of error in experimentation [1].

It is therefore important to take the restrained imperfection in the experimental modal parameters into account. First of all, the uncertainty of these parameters can be introduced into the modal updating process [2].

Another approach, which is proposed here, deals with the uncertainty earlier in the correction model process. The uncertainty is directly introduced into the experimental data (FRFs) in order to take it into account from the identification phase. The aim is also to provide a degree of confidence in the modal parameters identified.

Generally, imprecision is dealt with by stochastic approaches and in particular by Monte-Carlo simulations (MCS) [3–5]. Although these simulations are expensive in terms of CPU time, they are still the reference.

It is proposed to model uncertainties by fuzzy formalism [6] because it enables notions such as imprecision and uncertainty to be spread to more detailed descriptions such as vague, incomplete or linguistic quantities.

The development of the identification method is based on the LMA curve-fitting method [7].

After a brief theoretical review of this method, the uncertain experimental data modelled with fuzzy numbers is presented. This modelling will help to solve a non-linear system with fuzzy complex coefficients. Several solving techniques are discussed before proposing a method based on a first order Taylor development. Finally, the approach is illustrated with an academic test which, despite not reflecting a realistic situation, validates the method. The applied results are compared to those given by a Monte-Carlo approach.

2. DETERMINISTIC METHOD BASIS

According to the superposition modal principle, the response expression $y(t)$ of a forced harmonic excitation is given by:

$$y(t) = \left[\sum_{v=1}^n \frac{\Psi_v \Psi_v^t}{(j\omega - s_v)} + \sum_{v=1}^n \frac{\bar{\Psi}_v \bar{\Psi}_v^t}{(j\omega - \bar{s}_v)} \right] f(t). \quad (1)$$

This response is written on the n complex eigenvectors Ψ_v (with $\bar{\Psi}_v$ and \bar{s}_v the conjugated) of the damped structure. The eigenvalues s_v are complex too and are expressed as $s_v = -a_v w_v + jw_v$ with a_v the eigendamping and w_v the eigenfrequency of the associated conservative structure.

Modes are identified by working in a frequency interval that contains either one isolated mode or several neighbouring modes. The approximate dynamic response implicating the n included modes involved in this frequency interval is given by

$$y \approx u + (j\omega)v + \sum_{v=1}^n \frac{\Psi_v \Psi_v^t}{(j\omega - s_v)} f, \quad (2)$$

where u and v are an additional linear contribution representing the effect of modes outside the frequency interval studied. The curve-fitting technique principle then consists in finding for each sensor i , the $(2n + 2)$ parameters $\mathbf{q}_j = [u_i, v_i, (t_{vi}, s_{vi})_{v=1, \dots, n}]$ minimizing the non-linear function:

$$f(\mathbf{q}_j, w_k, y_i) = y_i(w_k) - \left[u_i + jw_k v_i + \sum_{v=1}^n \frac{t_{vi}}{(jw_k - s_{vi})} \right] \quad (3)$$

when $y_i(w_k)$ is the measured response on k th frequency in sensor i and $t_{vi} = \Psi_{vi} \Psi_v^t f$.

After first order linearization, a linear over-determined system which has unknown complex values is solved. The least-squares solution is given by

$$\bar{A}^T(\mathbf{q}_i) A(\mathbf{q}_i) d\mathbf{q}_i = \bar{A}^T(\mathbf{q}_i) \mathbf{b}(\mathbf{q}_i) \quad (4)$$

with $\mathbf{q}_{i+1} = \mathbf{q}_i + d\mathbf{q}_i$.

This system is solved by iteration for each sensor until convergence of the $(2n + 2)$ \mathbf{q}_j parameters.

3. UNCERTAINTY MEASURE MODELLING

The previous identification principle is a deterministic calculation exploiting the FRFs. However, in practice, the test conditions cannot generally be reproduced. So, in several sets of experimental tests, one observes in the FRFs a mode position shift in amplitude as much as in frequency. To take this shifting into account, it is proposed to model amplitudes and frequencies measured with fuzzy numbers.

This modelling is presented below on the measured response y_i and frequencies w_k .

3.1. FREQUENCIES UNCERTAINTY

The eigenfrequencies shifting observed in a FRF set is taken into account by introducing uncertainty into the measured frequencies (Figure 1).

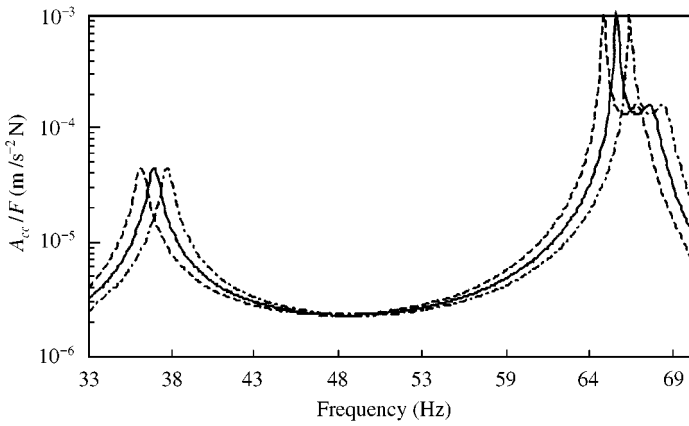


Figure 1. Frequency uncertainty representation for $\mu = 0$: —, measured response; ---, minimal response; - · - · maximal response.

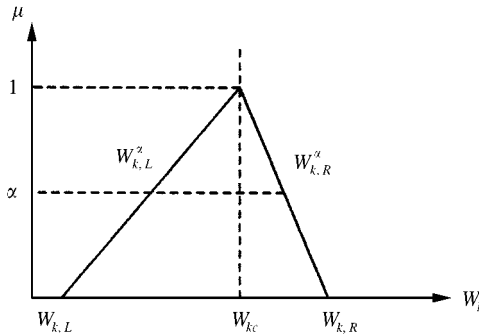


Figure 2. Fuzzy frequency \tilde{w}_k^α .

The uncertainty in measured frequencies is modelled by a fuzzy triangular number as shown in Figure 2.

The fuzzy frequency \tilde{w}_k^α is described by its membership function $\mu(\mu \in [0; 1])$ which is defined by levels called α -cuts [8]. The interval of confidence $[w_{k,L}^\alpha; w_{k,R}^\alpha]$ (L for left and R for right) is associated with each α -cut. The crisp value w_{kc} corresponds to the measurement and boundaries $[w_{k,L}; w_{k,R}]$ are obtained by uncertainty estimation on the measured frequencies.

For a fuzzy triangular number, the interval $[w_{k,L}^\alpha; w_{k,R}^\alpha]$ at the α -cut is given by:

$$\begin{aligned}
 w_{k,L}^\alpha &= w_{kc} + |w_{kc}| |\varepsilon_{w,L}| \left(\frac{\alpha}{N_\alpha} - 1 \right) \\
 w_{k,R}^\alpha &= w_{kc} + |w_{kc}| |\varepsilon_{w,R}| \left(1 - \frac{\alpha}{N_\alpha} \right)
 \end{aligned}
 \quad \text{with } \alpha \in [0; N_\alpha], \tag{5}$$

where $\varepsilon_{w,L}$ and $\varepsilon_{w,R}$ are the lower and upper percentages representative of the estimated error on the measured frequency. N_α is the number of α -cuts.

3.2. RESPONSE UNCERTAINTY

A fuzzy number for each sensor and each frequency using the same principle models the uncertain measured response. This modelling replicates the amplitude shifting observed on the FRFs set (Figure 3).

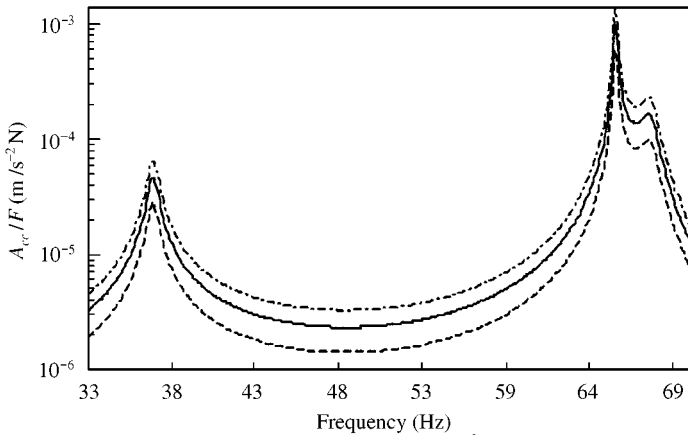


Figure 3. Amplitude uncertainty representation for $\mu = 0$: —, measured response; ---, minimal response; - · -, maximal response.

In the same way as in equation (5), the fuzzy response \tilde{y}_i^α of the sensor i is expressed by:

$$\begin{aligned}
 y_{i,L}^\alpha &= y_{ic} + |y_{ic}| |\varepsilon_{y,L}| \left(\frac{\alpha}{N_\alpha} - 1 \right) \\
 y_{i,R}^\alpha &= y_{ic} + |y_{ic}| |\varepsilon_{y,R}| \left(1 - \frac{\alpha}{N_\alpha} \right)
 \end{aligned}
 \quad \text{with } \alpha \in [0; N_\alpha], \tag{6}$$

where $\varepsilon_{y,L}$ and $\varepsilon_{y,R}$ are the lower and upper percentages representative of the estimated error on the measured response. N_α is the number of α -cuts and y_{ic} the crisp value results of the measurement.

4. PROBLEMATICS

Equation (3) is taken again but this time the FRFs are considered uncertain. The $(2n + 2)$ fuzzy parameters $\tilde{\mathbf{q}}_j^\alpha$ are therefore found which minimize the following expression:

$$f(\tilde{\mathbf{q}}_j^\alpha, \tilde{w}_k^\alpha, \tilde{y}_i^\alpha) = \tilde{y}_i^\alpha - \left[\tilde{u}_i^\alpha + j\tilde{w}_k^\alpha \tilde{v}_i^\alpha + \sum_{v=1}^n \frac{\tilde{t}_{vi}^\alpha}{(j\tilde{w}_k^\alpha - \tilde{s}_{vi}^\alpha)} \right] \tag{7}$$

to solve the fuzzy system after linearization as in equation (4):

$$\tilde{\mathbf{A}}_i^\alpha \mathbf{d}\tilde{\mathbf{q}}_i^\alpha = \tilde{\mathbf{b}}_i^\alpha, \tag{8}$$

with $\tilde{\mathbf{q}}_{i+1}^\alpha = \tilde{q}_i^\alpha + \mathbf{d}\tilde{\mathbf{q}}_i^\alpha$.

This system is an interval system with fuzzy complex coefficients. Various solutions are proposed and discussed.

4.1. SUCCESSIVE DETERMINISTIC SOLUTIONS

An initial simple approach to implement consists in solving the system (8) independently of each α -cut. A left-deterministic identification (for y_L^α, w_L^α) and a right-deterministic identification (for y_R^α, w_R^α) is achieved for each α -cut as described in section 2. The

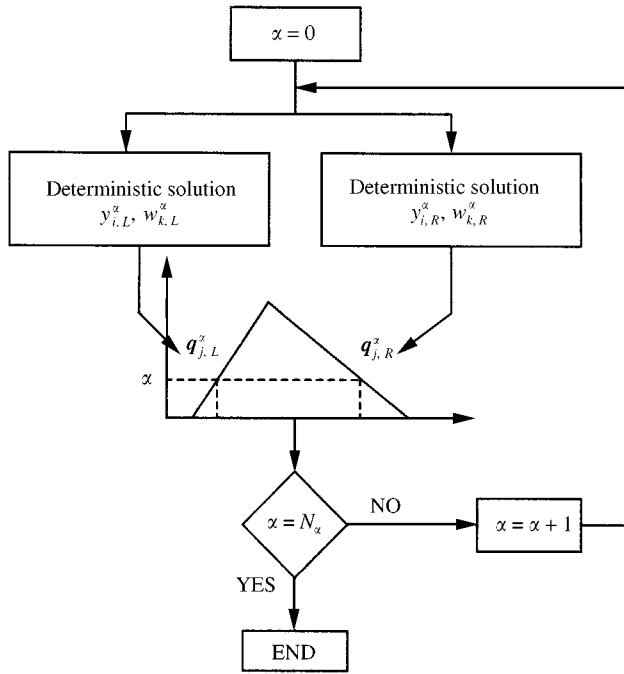


Figure 4. Successive deterministic solutions.

interval $[q_{j,L}^\alpha, q_{j,R}^\alpha]$ is associated with each solution set on an α -cut. The fuzzy vector \tilde{q}_j^α is obtained by taking into account all α -cuts according to the algorithm in Figure 4.

This method has two major disadvantages. It does not always respect either the convexity criteria or the order relation between the left and the right boundaries. These problems are due to the fact that left and right solutions are independent of the α -cuts. Besides, solutions for a given α -cut do not necessarily exist.

4.2. FUZZY ARITHMETIC APPLICATION

A second approach consists in using fuzzy numbers arithmetic in order to directly solve the fuzzy system (8). Traditionally, the interval system solution is given by the vertex method [9], which uses the “min” and “max” operators (see Appendix A). The application of this method therefore gives rise to some problems.

First of all, the fuzzy matrix \tilde{X}^α contains by constructions mixed fuzzy numbers, i.e., fuzzy numbers containing zero. The vertex method is not adapted to fuzzy operations on mixed fuzzy numbers because it generates discontinuities for some arithmetical operations as shown for the fuzzy division in the following example.

for $\tilde{X}^\alpha = [-1; 2; 3]$:

$$\frac{1}{\tilde{X}^\alpha} = \left[\min\left(\frac{1}{X_L^\alpha}; \frac{1}{X_R^\alpha}\right); \max\left(\frac{1}{X_L^\alpha}; \frac{1}{X_R^\alpha}\right) \right],$$

$$(\tilde{X}^\alpha)^2 = [\min(X_L^\alpha \cdot X_L^\alpha; X_L^\alpha \cdot X_R^\alpha; X_R^\alpha \cdot X_R^\alpha); \max(X_L^\alpha \cdot X_L^\alpha; X_L^\alpha \cdot X_R^\alpha; X_R^\alpha \cdot X_R^\alpha)]. \tag{9}$$

Figure 5 shows that the division on mixed fuzzy numbers defined by the vertex method generates discontinuity on the zero.

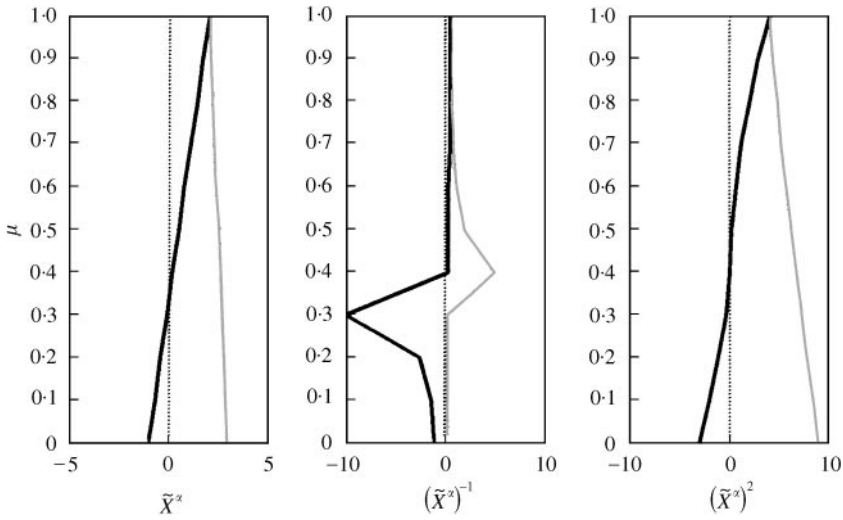


Figure 5. Operations on mixed fuzzy numbers: the vertex method.

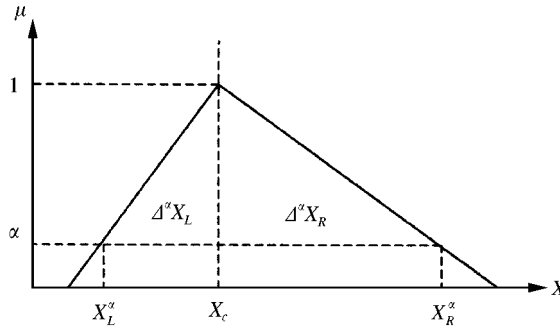


Figure 6. Illustration of the perturbation principle.

Otherwise, the system (8) is a complex system. It is therefore impossible to use the “min” and “max” operators of the vertex method because there is no order relation in \mathbb{C} .

A solution consists in using the perturbation principle to define fuzzy complex arithmetical operations (see Appendix B). The perturbation principle (Figure 6) consists in writing fuzzy numbers \tilde{X}^α for each α -cut as a variation (perturbation) in relation to its crisp value X_c as

$$\tilde{X}^\alpha = X_c + \Delta^\alpha X, \quad \text{with} \quad X_L^\alpha = X_c + \Delta^\alpha X_L, \quad \text{and} \quad X_R^\alpha = X_c + \Delta^\alpha X_R. \quad (10)$$

The fuzzy arithmetical operations can then be defined. The application to the example in Figure 5 gives the following solutions:

$$\frac{1}{\tilde{X}^\alpha} = \frac{1}{X_c} - \frac{\Delta^\alpha X}{(X_c)^2}, \quad (\tilde{X}^\alpha)^2 = (X_c)^2 + 2X_c \Delta^\alpha X. \quad (11)$$

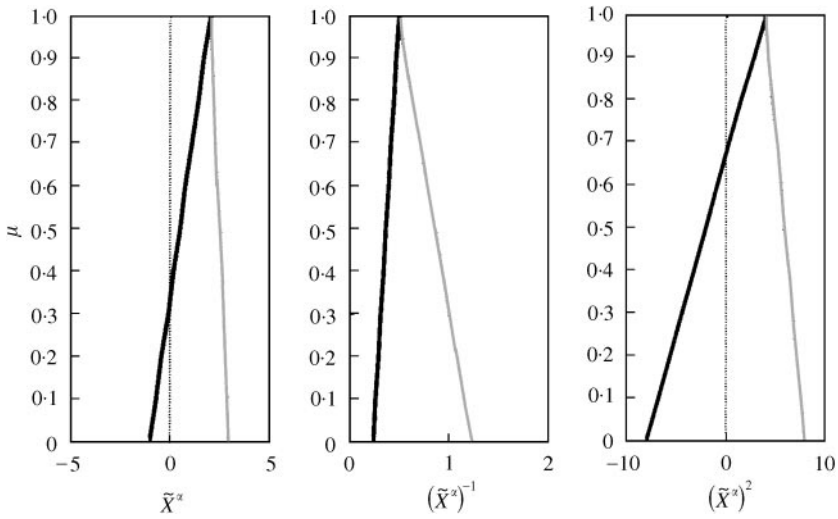


Figure 7. Operations on mixed fuzzy numbers: perturbation principle.

Figure 7 shows that operations on mixed fuzzy numbers defined by the perturbation method give convex solutions.

For fuzzy complex numbers, the fuzzy number will be broken up according to its real and imaginary parts as

$$\tilde{\mathbf{Z}}^x = \tilde{\mathbf{A}}^x + j\tilde{\mathbf{B}}^x = (\mathbf{A}_c + \Delta^x \mathbf{A}) + j(\mathbf{B}_c + \Delta^x \mathbf{B}). \tag{12}$$

One can then define all arithmetical operations on fuzzy complex numbers from this formulation and construct the system (8) components $\tilde{\mathbf{A}}^x$ and $\tilde{\mathbf{b}}^x$.

This system is solved by an iterative method. However, iterative schemes coupled with the fuzzy operations defined by the perturbation method generate problems on fuzzy number supports. Indeed evolution of the fuzzy numbers support is exponential during iterations. The fuzzy number support is its width interval base (for $\mu = 0$). The parameter's vector solution is also over-estimated.

In the light of these problems, an approach is proposed that uses the analogy between the perturbation principle and the first order Taylor development.

5. THE DIFFERENTIATION METHOD

5.1. PRINCIPLE

The writing formulation analogy between the perturbation principle and the first order Taylor development is described here.

For a given function $f(x)$, according to the perturbation principle, the fuzzy function \tilde{f}^x associated with the fuzzy number \tilde{x}^x is written as follows:

$$\tilde{f}^x = f_c + \Delta^x f. \tag{13}$$

The first order development of the function $f(x)$ around the point x_0 is expressed by:

$$f(x) = f(x_0) + \left. \frac{\partial f(x)}{\partial x} \right|_{x_0} dx + \varepsilon. \tag{14}$$

The formulations (13) and (14) for $x_0 = x_c$ gives

$$f_c = f(x_c)$$

$$\Delta^\alpha f = \left. \frac{\partial f(x)}{\partial x} \right|_{x_c} dx \approx \left. \frac{\partial f(x)}{\partial x} \right|_{x_c} \Delta^\alpha x. \tag{15}$$

5.2. SOLVING THE SYSTEM

It is proposed here to use this analogy to solve the fuzzy identification problem. The method consists of writing the fuzzy function (7) as the first order development of the deterministic function (3) according to the uncertain parameters around their crisp values (deterministic).

The uncertain parameters are the measured responses \tilde{y}_i^α ; the measured frequencies $\tilde{w}_k^\alpha = 2\pi\tilde{f}_k^\alpha$; the unknown parameters $\tilde{\mathbf{q}}_j^\alpha = [\tilde{u}_i^\alpha, \tilde{v}_i^\alpha, (\tilde{t}_{vi}^\alpha, \tilde{s}_{vi}^\alpha)_{v=1, \dots, n}]$.

Then the first order development gives

$$f(\tilde{\mathbf{q}}_j^\alpha, \tilde{w}_k^\alpha, \tilde{y}_i^\alpha) = f(\mathbf{q}_{jc}, w_{kc}, y_{ic}) + \left. \frac{\partial f}{\partial \mathbf{q}_j} \right|_{f_c} \Delta^\alpha \mathbf{q}_j + \left. \frac{\partial f}{\partial y_i} \right|_{f_c} \Delta^\alpha y_i + \left. \frac{\partial f}{\partial w_k} \right|_{f_c} \Delta^\alpha w_k + \varepsilon. \tag{16}$$

The perturbation principle (13) analogy gives

$$f_c = f(\mathbf{q}_{jc}, w_{kc}, y_{ic}), \tag{17}$$

$$\Delta^\alpha f = \left. \frac{\partial f}{\partial \mathbf{q}_j} \right|_{f_c} \Delta^\alpha \mathbf{q}_j + \left. \frac{\partial f}{\partial y_i} \right|_{f_c} \Delta^\alpha y_i + \left. \frac{\partial f}{\partial w_k} \right|_{f_c} \Delta^\alpha w_k + \varepsilon. \tag{18}$$

This system is solved in two stages. First of all, equation (17) is solved which corresponds to the deterministic calculation shown in section 2. The solution gives the crisp values of the $\tilde{\mathbf{q}}_j^\alpha$ parameters.

Equation (18) solution then determines the parameters' variations $\Delta^\alpha \mathbf{q}_j$. As this system is linear, it is solved in as much time as there are α -cuts.

For each sensor i , the equation system (18) formulation is:

$$\begin{bmatrix} 1 & jw_{1c} & \frac{1}{(jw_{1c} - s_{1ic})} & \frac{t_{1ic}}{(jw_{1c} - s_{1ic})^2} & \dots & \frac{1}{(jw_{1c} - s_{nic})} & \frac{t_{nic}}{(jw_{1c} - s_{nic})^2} \\ \vdots & \vdots & \vdots & \vdots & & \vdots & \vdots \\ 1 & jw_{kc} & \frac{1}{(jw_{kc} - s_{1ic})} & \frac{t_{1ic}}{(jw_{kc} - s_{1ic})^2} & \dots & \frac{1}{(jw_{kc} - s_{nic})} & \frac{t_{nic}}{(jw_{kc} - s_{nic})^2} \\ \vdots & \vdots & \vdots & \vdots & & \vdots & \vdots \\ 1 & jw_{pc} & \frac{1}{(jw_{pc} - s_{1ic})} & \frac{t_{1ic}}{(jw_{pc} - s_{1ic})^2} & \dots & \frac{1}{(jw_{pc} - s_{nic})} & \frac{t_{nic}}{(jw_{pc} - s_{nic})^2} \end{bmatrix} \begin{bmatrix} \Delta^\alpha u_i \\ \Delta^\alpha v_i \\ \Delta^\alpha t_{1i} \\ \Delta^\alpha s_{1i} \\ \vdots \\ \Delta^\alpha t_{ni} \\ \Delta^\alpha s_{ni} \end{bmatrix}$$

$$= \begin{bmatrix} \Delta^\alpha y_i(w_{1c}) + \left[-jv_{ic} + \sum_{v=1}^n \frac{j t_{vic}}{(jw_{1c} - s_{vic})^2} \right] \Delta^\alpha w_1 \\ \vdots \\ \Delta^\alpha y_i(w_{kc}) + \left[-jv_{ic} + \sum_{v=1}^n \frac{j t_{vic}}{(jw_{kc} - s_{vic})^2} \right] \Delta^\alpha w_k \\ \vdots \\ \Delta^\alpha y_i(w_{pc}) + \left[-jv_{ic} + \sum_{v=1}^n \frac{j t_{vic}}{(jw_{pc} - s_{vic})^2} \right] \Delta^\alpha w_p \end{bmatrix} + \varepsilon \quad (19)$$

which gives

$$\mathbf{A} \Delta^\alpha \mathbf{q}_j = \Delta^\alpha \mathbf{b} + \varepsilon. \quad (20)$$

The matrix \mathbf{A} and intervals' vector $\Delta^\alpha \mathbf{b}$ are constructed from parameters $\tilde{\mathbf{q}}_j^\alpha$ crisp values identified previously by the solution of equation (17) and variations $\Delta^\alpha y_i$ and $\Delta^\alpha w_k$ representing measurement uncertainty as defined in section 3. This system (20) is an over-determinate complex system with $\Delta^\alpha \mathbf{q}_j$ and $\Delta^\alpha \mathbf{b}$ intervals' vectors.

To be able to solve the system, it is broken up according to its real and imaginary parts. According to the perturbation principle, the system can be written as

$$[\mathbf{A}_r + j\mathbf{A}_i] [\Delta^\alpha \mathbf{q}_r + j\Delta^\alpha \mathbf{q}_i] = [\Delta^\alpha \mathbf{b}_r + j\Delta^\alpha \mathbf{b}_i] \quad (21)$$

while keeping only first order terms:

$$\begin{bmatrix} \mathbf{A}_r & | & -\mathbf{A}_i \\ \hline -\mathbf{A}_i & | & \mathbf{A}_r \end{bmatrix} \begin{bmatrix} \Delta^\alpha \mathbf{q}_r \\ \Delta^\alpha \mathbf{q}_i \end{bmatrix} = \begin{bmatrix} \Delta^\alpha \mathbf{b}_r \\ \Delta^\alpha \mathbf{b}_i \end{bmatrix}. \quad (22)$$

$$\mathbf{\Pi} \quad \Delta^\alpha \mathbf{Q} = \Delta^\alpha \mathbf{B}$$

The interval calculation gives the parameters' variations $\Delta^\alpha \mathbf{q}_j$ solution of this new real intervals' system. For each α -cut one solves

$$\begin{aligned} \Delta^\alpha \mathbf{Q}_L &= \min [(\mathbf{\Pi}^t \mathbf{\Pi})^{-1} \mathbf{\Pi}^t \Delta^\alpha \mathbf{B}_L, (\mathbf{\Pi}^t \mathbf{\Pi})^{-1} \mathbf{\Pi}^t \Delta^\alpha \mathbf{B}_R], \\ \Delta^\alpha \mathbf{Q}_R &= \max [(\mathbf{\Pi}^t \mathbf{\Pi})^{-1} \mathbf{\Pi}^t \Delta^\alpha \mathbf{B}_L, (\mathbf{\Pi}^t \mathbf{\Pi})^{-1} \mathbf{\Pi}^t \Delta^\alpha \mathbf{B}_R]. \end{aligned} \quad (23)$$

Fuzzy parameters $\tilde{\mathbf{q}}_j^\alpha$ are constructed with the crisp values \mathbf{q}_{jc} , solution of system (17) and the variations $\Delta^\alpha \mathbf{q}_j$, solution of system (22) as

$$\tilde{\mathbf{q}}_j^\alpha = \mathbf{q}_{jc} + \Delta^\alpha \mathbf{q}_j. \quad (24)$$

One then knows the fuzzy complex eigenvalues $\tilde{\mathbf{s}}_v^\alpha$ and the fuzzy eigenvectors $\tilde{\mathbf{\Psi}}_{vi}^\alpha$.

It is therefore possible to quantify uncertainty and also provide a degree of confidence from these identified parameters with operators such as area, entropy or specificity [10].

5.3. ALGORITHM

Figure 8 presents the algorithm used.

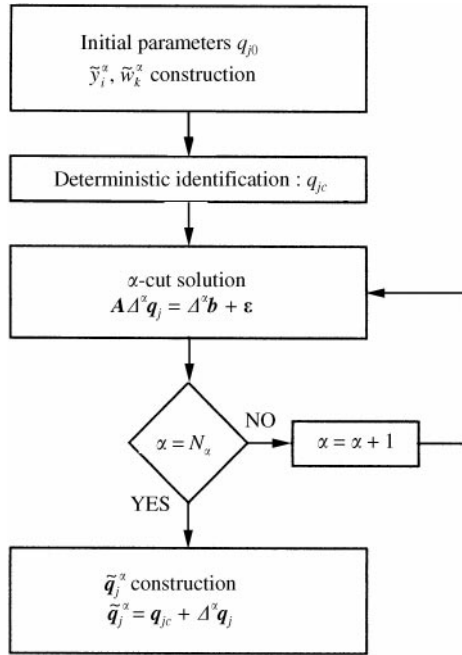


Figure 8. Algorithm.

6. APPLICATION

The proposed method is applied to identify the uncertain modal parameters of a mechanical system with three degrees of freedom (Figure 9).

There are FRFs from three sensors to proceed to the mode identification of this structure. These FRFs show the presence of three modes (Figure 10).

The uncertainty measurement is considered here by the FRFs shifting in amplitudes as much as in frequencies. These uncertainties are modelled with fuzzy numbers as shown in section 3. The lower and upper estimations of error percentage is 20% on amplitudes and 0.5% on frequencies.

Tables 1–3 present the defuzzified eigensolutions (eigenfrequencies, eigendamping and eigenvectors), a result of the fuzzy identification for the three identified modes. These results are then compared with the theoretical eigensolutions and the mean values of a MCS.

Since fuzzy numbers are symmetrical around their crisp value, defuzzified numbers correspond to those crisp values.

Assuming Gaussian distributions, results from Monte-Carlo analysis are characterized by their mean value and standard deviation (m, σ). The interval $[m - 3\sigma; m + 3\sigma]$ represents an interval of confidence of 97.5%. The associated fuzzy number is also defined as shown in Figure 11, the crisp value is given by the mean value m and the boundaries by $[m + \Delta m_L; m + \Delta m_R]$ with $\Delta m_L = -3\sigma$ and $\Delta m_R = 3\sigma$.

Generally, CPU time cost is in favour of fuzzy arithmetic. For fuzzy arithmetic, the CPU time depends on the number of α -cuts and as an example with symmetrical triangular fuzzy numbers, two α -cuts are sufficient (one for the crisp value and one for the boundaries). This needs only a deterministic and two variations calculus. But if one wants a good discretization of the shape function (π shape for example), the number of α -cuts must be notably increased and CPU time too. For MCS, the CPU time depends on the

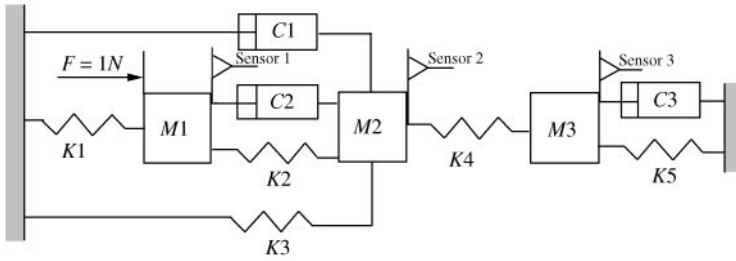


Figure 9. Test structure $M1 = 6 \text{ Kg}$; $M2 = 0.5 \text{ Kg}$; $M3 = 0.08 \text{ Kg}$; $K1 = 1 \times 10^6 \text{ N/m}$; $K2 = 1.3 \times 10^4 \text{ N/m}$; $K3 = 2 \times 10^4 \text{ N/m}$; $K4 = 1.1 \times 10^4 \text{ N/m}$; $K5 = 500 \text{ N/m}$; $C1 = 0.7 \text{ Ns/m}$; $C2 = 0.4 \text{ Ns/m}$; $C3 = 0.7 \text{ Ns/m}$.

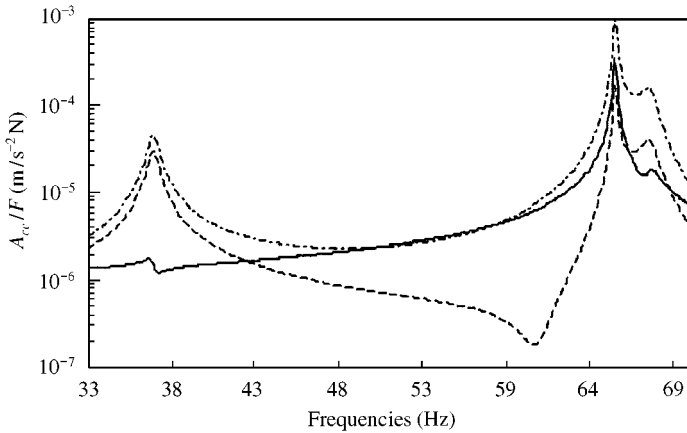


Figure 10. FRFs test structure: —, sensor 1; ---, sensor 2; - · -, sensor 3.

TABLE 1

First-mode eigenvalues

Mode 1	Theoretical values	Defuzzified values	MCS means values
Frequency	36.94 Hz	36.936 Hz	36.935 Hz
Damping	0.851%	0.851%	0.880%
Vector sensor 1	$0.758^{E-03} - 0.731^{E-03}i$	$0.757^{E-03} - 0.732^{E-03}i$	$0.763^{E-03} - 0.736^{E-03}i$
Vector sensor 2	$0.397^{E-01} - 0.394^{E-0.1}i$	$0.397^{E-01} - 0.394^{E-01}i$	$0.399^{E-01} - 0.395^{E-01}i$
Vector sensor 3	$0.599^{E-0.1} - 0.610^{E-01}i$	$0.599^{E-01} - 0.610^{E-01}i$	$0.603^{E-01} - 0.612^{E-01}i$

TABLE 2

Second-mode eigenvalues

Mode 2	Theoretical values	Defuzzified values	MCS means values
Frequency	65.18 Hz	65.1784 Hz	65.1771 Hz
Damping	0.126%	0.125%	0.184%
Vector sensor 1	$0.975^{E-02} - 0.915^{E-02}i$	$0.974^{E-02} - 0.915^{E-02}i$	$0.971^{E-02} - 0.927^{E-02}i$
Vector sensor 2	$0.329^{E-02} - 0.655^{E-02}i$	$0.329^{E-02} - 0.655^{E-02}i$	$0.325^{E-02} - 0.661^{E-02}i$
Vector sensor 3	$-0.234^{E-01} + 0.345^{E-01}i$	$-0.234^{E-01} + 0.345^{E-01}i$	$-0.232^{E-01} + 0.348^{E-01}i$

TABLE 3
Third-mode eigenvalues

Mode 3	Theoretical values	Defuzzified values	MCS means values
Frequency	67.33 Hz	67.333 Hz	67.183 Hz
Damping	0.714%	0.714%	0.992%
Vector sensor 1	$0.273^{E-02} - 0.432^{E-02}i$	$0.273^{E-02} - 0.432^{E-02}i$	$0.477^{E-02} - 0.304^{E-02}i$
Vector sensor 2	$0.176^{E-01} - 0.173^{E-01}i$	$-0.176^{E-01} - 0.173^{E-01}i$	$-0.195^{E-01} + 0.123^{E-01}i$
Vector sensor 3	$0.707^{E-01} - 0.650^{E-01}i$	$0.707^{E-01} - 0.650^{E-01}i$	$0.472^{E-01} - 0.478^{E-01}i$

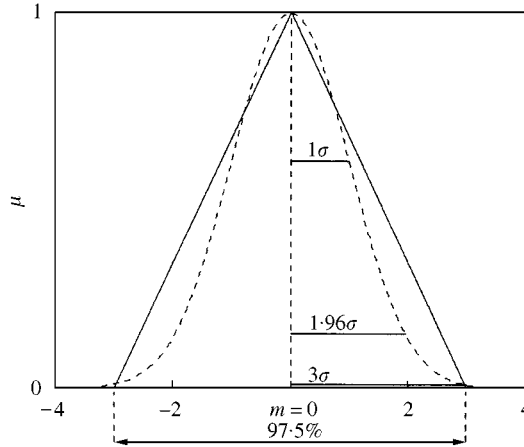


Figure 11. Fuzzy representation from Monte-Carlo results: ---, Gaussian distribution; — associated fuzzy number.

TABLE 4
Left, crisp and right values for eigenfrequencies (Hz)

Mode	Left	Crisp	Right	Uncertainty area
1	36.9218	36.936	36.9503	0.01425
2	65.1629	65.1784	65.1938	0.01545
3	67.026	67.333	67.6399	0.30695

wanted precision on the mean value or on the standard deviation. Naturally, the precision is better and the calculus were expensive. Otherwise, a good precision on standard deviation is more suitable but is also more expensive. In the present application, fuzzy analysis was achieved in 10s CPU with 10 α -cuts and Monte-Carlo analysis was achieved in 6443 s CPU (5500 simulations for a precision of 10^{-4} on mean value and 10^{-3} on standard deviation).

A very good correlation between the theoretical and defuzzified identification solutions are noted.

The fuzzy identification method is also capable of quantifying the uncertainty of identified eigenvalues and providing an interval of confidence as shown in Table 4 for the eigenfrequencies. The uncertainty criterion is the area of fuzzy triangular numbers.

As it was predictable, note that the most important uncertainty on the eigenfrequencies is located on the third mode. Indeed, the fuzzy identification was chosen to be applied to this simple case because the deterministic identification behaviour of this structure is known. In the deterministic case, identification of the first two modes is easy but it is more complex for identification of the third mode because it is coupled with the second. The fuzzy identification behaviour clearly illustrates this tendency.

It is the same with the uncertainty area of the other eigenvalues as shown in Figure 12. The third mode eigensolutions are more sensitive to the uncertain measurement than those of the two other modes.

Otherwise, one notes a very good correlation of the eigensolutions uncertainty area between the fuzzy and the MCS approaches.

Although qualitative results are in agreement with the fuzzy identification and MCS approaches, there are nevertheless differences with the quantitative results. Indeed,

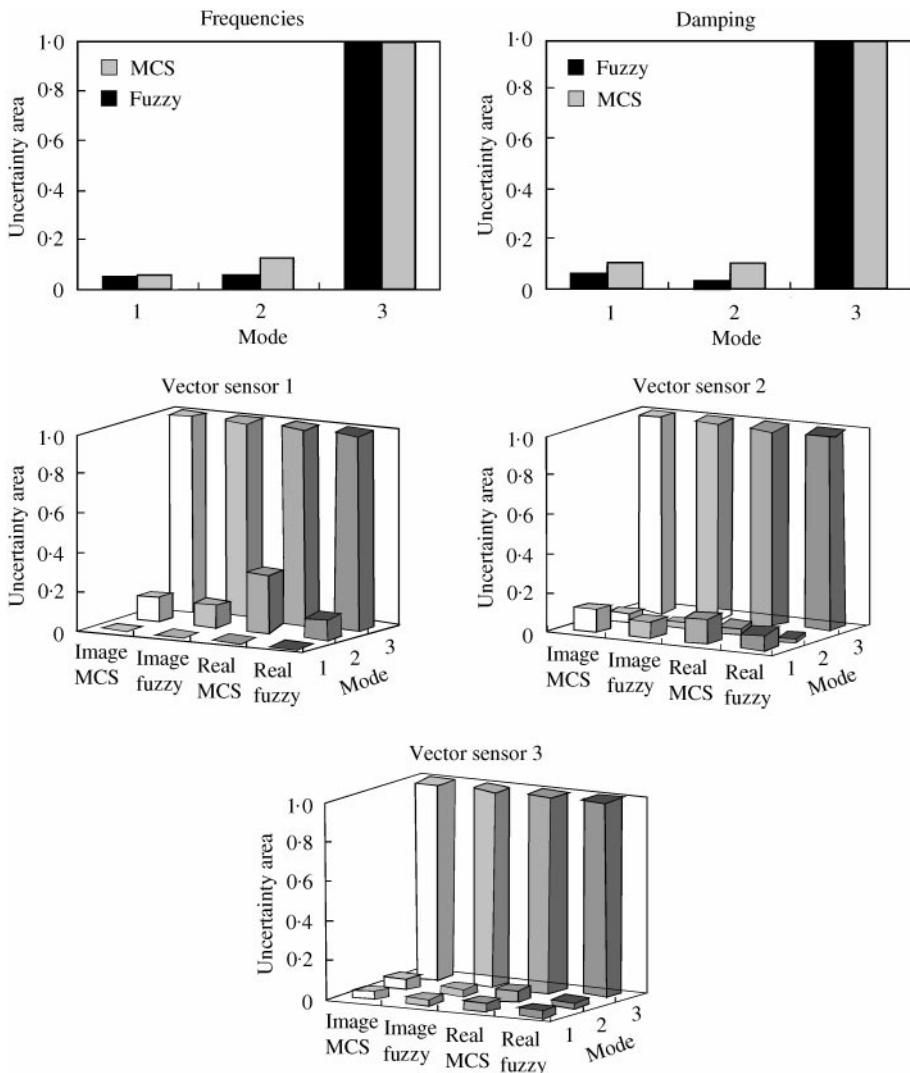


Figure 12. Eigensolutions normalized uncertainty ■; fuzzy; □; MCS.

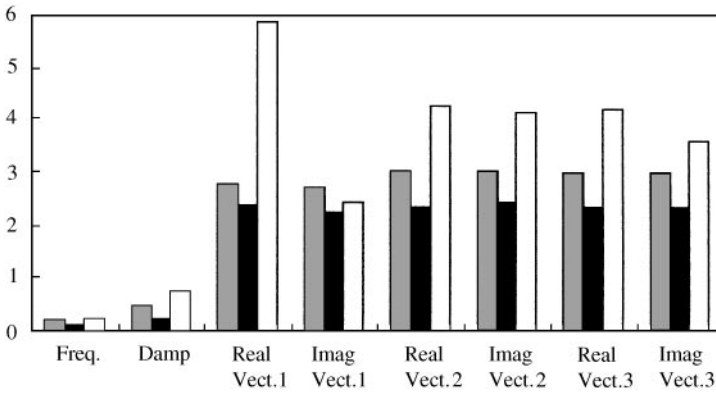


Figure 13. Uncertainties ratio fuzzy/SMC: ■ Mode 1; ■ Mode 2; □ Mode 3.

comparison of the fuzzy identification and MCS quantitative results shows that the uncertainty of the fuzzy identification is under-valued in relation to that of the MCS for eigenfrequencies and eigendamping while it appears to be overvalued for the eigenvectors. This phenomenon is underlined by Figure 13 which presents the uncertainties ratio between the fuzzy identification and the MCS results.

7. CONCLUSION

A modal identification method has been proposed which takes uncertainty on experimental data into account. This uncertainty is modelled by fuzzy numbers. Difficulties in solving a fuzzy system have been discussed and an alternative method based on the first order Taylor development was proposed to solve such system. Finally, the application to a simple system and the comparison with MCS results validated the approach and therefore provided a degree of confidence in the modal parameters identified.

ACKNOWLEDGMENTS

The present research work has been supported by the CNRS, the European Community, the Conseil Régional Nord-Pas de Calais, the Ministère de l'Education Nationale, the Délégation Régionale à la Recherche et à la Technologie. The authors gratefully acknowledge the support of these institutions.

REFERENCES

1. M. LINK 1990 *Proceedings of the 8th International Modal Analysis Conference, Kissimmee, Florida*, Vol. 1, 570–578. Identification and correction of errors in analytical models using test data—theoretical and practical bounds.
2. A. CHERKI 1998 *Thesis, University of Valenciennes France*. Prise en compte des imprécisions de modélisation en calculs des structures.
3. A. PIERRIOT, J. L. RAYNAUD and S. COGAN 1998 *Proceedings of the 23rd International Symposium of Modal Analysis, Leuven, Belgium*, Vol. 2, 953–960. Uncertainties in identified modal parameters.
4. J. E. LEE and S. D. FASSOIS 1993 *Journal of sound and vibration* **161**, 33–87. On the problem of stochastic experimental modal analysis based on multiple-excitation multiple-response data—Parts I and II.

5. P. GUILLAUME, P. VERBOVEN and S. VANLANDUIT 1998 *Proceedings of the 23rd International Symposium of Modal Analysis, Leuven, Belgium*, Vol. 1, 359–366. Frequency domain maximum likelihood identification of modal parameters with confidence intervals.
6. L. A. ZADEH 1978 *Fuzzy Sets and Systems* **1**, 3–28. Fuzzy sets as a basis for a theory of possibility.
7. R. FILLOD, G. LALLEMAND, J. PIRANDA and J. L. RAYNAUD 1989 *Manuel théorique, Laboratoire de Mécanique Appliquée de Besançon*. Notice d'utilisation du programme MODAN PC.
8. J. J. BUCKLEY and Y. QU 1990 *Fuzzy Sets and Systems* **38**, 309–312. On using α -cuts to evaluate fuzzy equations.
9. W. DONG and H. C. SHAH 1987 *Fuzzy Sets and Systems* **24**, 65–78. Vertex method for computing functions of fuzzy variables.
10. A. KAUFMANN 1977 *Introduction à la théorie des sous ensembles flous*. Paris: Masson.

APPENDIX A: VERTEX INTERVAL COMPUTATION

$$\text{Addition: } [a_L^\alpha; a_R^\alpha] + [b_L^\alpha; b_R^\alpha] = [a_L^\alpha + b_L^\alpha; a_R^\alpha + b_R^\alpha]. \quad (\text{A1})$$

$$\text{Subtraction: } [a_L^\alpha; a_R^\alpha] - [b_L^\alpha; b_R^\alpha] = [a_L^\alpha - b_R^\alpha; a_R^\alpha - b_L^\alpha]. \quad (\text{A2})$$

$$\begin{aligned} \text{Multiplication: } [a_L^\alpha; a_R^\alpha] \times [b_L^\alpha; b_R^\alpha] = & [\min(a_L^\alpha, b_L^\alpha, a_L^\alpha \cdot b_R^\alpha, a_R^\alpha \cdot b_L^\alpha, a_R^\alpha \cdot b_R^\alpha); \\ & \max(a_L^\alpha, b_L^\alpha, a_L^\alpha \cdot b_R^\alpha, a_R^\alpha \cdot b_L^\alpha, a_R^\alpha \cdot b_R^\alpha)]. \quad (\text{A3}) \end{aligned}$$

$$\begin{aligned} \text{Division: } [a_L^\alpha; a_R^\alpha] / [b_L^\alpha; b_R^\alpha] = & [\min(a_L^\alpha/b_L^\alpha, a_L^\alpha/b_R^\alpha, a_R^\alpha/b_L^\alpha, a_R^\alpha/b_R^\alpha); \\ & \max(a_L^\alpha/b_L^\alpha, a_L^\alpha/b_R^\alpha, a_R^\alpha/b_L^\alpha, a_R^\alpha/b_R^\alpha)]. \quad (\text{A4}) \end{aligned}$$

APPENDIX B: PERTURBATION INTERVAL COMPUTATION

B.1. COMPLEX INTERVALS

Fuzzy complex numbers are broken up according to their real and imaginary parts. Real interval arithmetic is then applied separately to the real and imaginary parts.

$$\text{Addition: } \tilde{A}^\alpha + \tilde{B}^\alpha = (\tilde{a}^\alpha + i\tilde{b}^\alpha) + (\tilde{c}^\alpha + i\tilde{d}^\alpha) = \tilde{C}^\alpha = (\tilde{e}^\alpha + i\tilde{f}^\alpha), \quad (\text{B1})$$

$$\tilde{e}^\alpha = \tilde{a}^\alpha + \tilde{c}^\alpha, \quad \tilde{f}^\alpha = \tilde{b}^\alpha + \tilde{d}^\alpha. \quad (\text{B2})$$

$$\text{Subtraction: } \tilde{A}^\alpha - \tilde{B}^\alpha = (\tilde{a}^\alpha + i\tilde{b}^\alpha) - (\tilde{c}^\alpha + i\tilde{d}^\alpha) = \tilde{C}^\alpha = (\tilde{e}^\alpha + i\tilde{f}^\alpha), \quad (\text{B3})$$

$$\tilde{e}^\alpha = \tilde{a}^\alpha - \tilde{c}^\alpha, \quad \tilde{f}^\alpha = \tilde{b}^\alpha - \tilde{d}^\alpha. \quad (\text{B4})$$

$$\text{Multiplication: } \tilde{A}^\alpha \times \tilde{B}^\alpha = (\tilde{a}^\alpha + i\tilde{b}^\alpha) \cdot (\tilde{c}^\alpha + i\tilde{d}^\alpha) = \tilde{C}^\alpha = (\tilde{e}^\alpha + i\tilde{f}^\alpha), \quad (\text{B5})$$

$$\tilde{e}^\alpha = \tilde{a}^\alpha \cdot \tilde{c}^\alpha - \tilde{b}^\alpha \cdot \tilde{d}^\alpha, \quad \tilde{f}^\alpha = \tilde{a}^\alpha \cdot \tilde{d}^\alpha + \tilde{b}^\alpha \cdot \tilde{c}^\alpha. \quad (\text{B6})$$

$$\text{Division: } \tilde{A}^\alpha / \tilde{B}^\alpha = (\tilde{a}^\alpha + i\tilde{b}^\alpha) / (\tilde{c}^\alpha + i\tilde{d}^\alpha) = \tilde{C}^\alpha = (\tilde{e}^\alpha + i\tilde{f}^\alpha), \quad (\text{B7})$$

$$\tilde{e}^\alpha = (\tilde{a}^\alpha \cdot \tilde{c}^\alpha + \tilde{b}^\alpha \cdot \tilde{d}^\alpha) / (\tilde{c}^{\alpha 2} + \tilde{d}^{\alpha 2}), \quad \tilde{f}^\alpha = (\tilde{b}^\alpha \cdot \tilde{c}^\alpha - \tilde{a}^\alpha \cdot \tilde{d}^\alpha) / (\tilde{c}^{\alpha 2} + \tilde{d}^{\alpha 2}). \quad (\text{B8})$$

B.2. REAL INTERVALS

$$\text{Addition: } \tilde{\mathbf{A}}^z + \tilde{\mathbf{B}}^z = (\mathbf{A}_c + \Delta^z \mathbf{A}) + (\mathbf{B}_c + \Delta^z \mathbf{B}) = (\mathbf{C}_c + \Delta^z \mathbf{C}), \quad (\text{B9})$$

$$\mathbf{C}_c = \mathbf{A}_c + \mathbf{B}_c, \quad \Delta^z \mathbf{C}_L = \Delta^z \mathbf{A}_L + \Delta^z \mathbf{B}_L, \quad \Delta^z \mathbf{C}_R = \Delta^z \mathbf{A}_R + \Delta^z \mathbf{B}_R. \quad (\text{B10})$$

$$\text{Subtraction: } \tilde{\mathbf{A}}^z - \tilde{\mathbf{B}}^z = (\mathbf{A}_c + \Delta^z \mathbf{A}) - (\mathbf{B}_c + \Delta^z \mathbf{B}) = (\mathbf{C}_c + \Delta^z \mathbf{C}), \quad (\text{B11})$$

$$\mathbf{C}_c = \mathbf{A}_c - \mathbf{B}_c, \quad \Delta^z \mathbf{C}_L = \Delta^z \mathbf{A}_L - \Delta^z \mathbf{B}_R, \quad \Delta^z \mathbf{C}_R = \Delta^z \mathbf{A}_R - \Delta^z \mathbf{B}_L. \quad (\text{B12})$$

$$\text{Multiplication: } \tilde{\mathbf{A}}^z \times \tilde{\mathbf{B}}^z = (\mathbf{A}_c + \Delta^z \mathbf{A}) \cdot (\mathbf{B}_c + \Delta^z \mathbf{B}) = (\mathbf{C}_c + \Delta^z \mathbf{C}), \quad (\text{B13})$$

$$\mathbf{C}_c = \mathbf{A}_c \cdot \mathbf{B}_c,$$

$$\Delta^z \mathbf{C}_L = \min(\mathbf{A}_c \Delta^z \mathbf{B}_L + \mathbf{B}_c \Delta^z \mathbf{A}_L; \mathbf{A}_c \Delta^z \mathbf{B}_R + \mathbf{B}_c \Delta^z \mathbf{A}_L;$$

$$\mathbf{A}_c \Delta^z \mathbf{B}_L + \mathbf{B}_c \Delta^z \mathbf{A}_R; \mathbf{A}_c \Delta^z \mathbf{B}_R + \mathbf{B}_c \Delta^z \mathbf{A}_R),$$

$$\Delta^z \mathbf{C}_R = \max(\mathbf{A}_c \Delta^z \mathbf{B}_L + \mathbf{B}_c \Delta^z \mathbf{A}_L; \mathbf{A}_c \Delta^z \mathbf{B}_R + \mathbf{B}_c \Delta^z \mathbf{A}_L;$$

$$\mathbf{A}_c \Delta^z \mathbf{B}_L + \mathbf{B}_c \Delta^z \mathbf{A}_R; \mathbf{A}_c \Delta^z \mathbf{B}_R + \mathbf{B}_c \Delta^z \mathbf{A}_R). \quad (\text{B14})$$

$$\text{Division: } \tilde{\mathbf{A}}^z / \tilde{\mathbf{B}}^z = (\mathbf{A}_c + \Delta^z \mathbf{A}) / (\mathbf{B}_c + \Delta^z \mathbf{B}) = (\mathbf{C}_c + \Delta^z \mathbf{C}), \quad (\text{B15})$$

$$\mathbf{C}_c = \mathbf{A}_c / \mathbf{B}_c,$$

$$\Delta^z \mathbf{C}_L = \min[(\mathbf{B}_c \Delta^z \mathbf{A}_L - \mathbf{A}_c \Delta^z \mathbf{B}_L) / \mathbf{B}_c^2; (\mathbf{B}_c \Delta^z \mathbf{A}_L - \mathbf{A}_c \Delta^z \mathbf{B}_R) / \mathbf{B}_c^2;$$

$$(\mathbf{B}_c \Delta^z \mathbf{A}_R - \mathbf{A}_c \Delta^z \mathbf{B}_L) / \mathbf{B}_c^2; (\mathbf{B}_c \Delta^z \mathbf{A}_R - \mathbf{A}_c \Delta^z \mathbf{A}_R) / \mathbf{B}_c^2],$$

$$\Delta^z \mathbf{C}_R = \max[(\mathbf{B}_c \Delta^z \mathbf{A}_L - \mathbf{A}_c \Delta^z \mathbf{B}_L) / \mathbf{B}_c^2; (\mathbf{B}_c \Delta^z \mathbf{A}_L - \mathbf{A}_c \Delta^z \mathbf{B}_R) / \mathbf{B}_c^2;$$

$$(\mathbf{B}_c \Delta^z \mathbf{A}_R - \mathbf{A}_c \Delta^z \mathbf{B}_L) / \mathbf{B}_c^2; (\mathbf{B}_c \Delta^z \mathbf{A}_R - \mathbf{A}_c \Delta^z \mathbf{A}_R) / \mathbf{B}_c^2]. \quad (\text{B16})$$